ELSEVIER

Journal of Molecular Catalysis A: Chemical 166 (2001) 31–38

JOURNAL OF MOLECULAR CATALYSIS A: CHEMICAL

www.elsevier.com/locate/molcata

The role of tungsten in formation of active sites for no SCR on the V-W-O catalyst surface — quantum chemical modeling (DFT)

E. Broclawik [a,*], A. Góra [b], M. Najbar [b]

[a] *Institute of Catalysis, Polish Academy of Sciences, Niezapominajek 8, 30239 Kraków, Poland*
[b] *Department of Chemistry, Jagiellonian University, 30060 Kraków, Ingardena 3, Poland*

Abstract

This study concerns quantum chemical modeling of water behavior on basal surface of WO_3–V_2O_5 solid solution crystallites with V_2O_5 structure. It was undertaken in order to validate the hypothesis that the presence of W atoms in vanadia-like surface species of V-W-O catalysts facilitates low temperature water dissociation leading to formation of OH groups being active sites in selective NO_x reduction by ammonia. Quantum chemical calculations were done with the use of modern electronic structure methodology based on the density functional theory (DFT). The calculations were performed for small clusters representing two adjacent metal sites in pentacoordinated oxygen environment, analogous to bipiramidal clusters introduced in description of the basal face of vanadium pentoxide. The results indicate that adsorption of water strongly depends on the presence of tungsten atom at the surface. Dissociative water adsorption leading to Bronsted acid centers creation is promoted. The proton acidity of the centers decreases with the increase of tungsten concentration in V_2O_5 matrix leading to the increase of $V^{4+}W^{6+}/V^{5+}W^{6+}$ ratio.

Keywords: DFT; WO_3–V_2O_5 solid solution; Water adsorption

1. Introduction

Vanadium pentoxide is one of the most popular active compounds in heterogeneous catalysis. Catalysts based on V_2O_5 show excellent catalytic properties important in selective oxidation of hydrocarbons and in selective catalytic reduction (SCR) of nitrogen oxides by ammonia. According to Busca et al. [1] the mechanism of SCR process is still uncompleted. There is a general agreement on the fact that the active sites are connected with the vanadium ions and that strong adsorption of ammonia is necessary for NO conversion. Adsorption data show that ammonia activation could occur on Lewis acid sites, on vanadyl groups or on V–OH Bronsted acid sites. Mechanisms of SCR reactions proposed by Janssen et al. [2] is related to V=O groups; this claimed by Ramis et al. [3] to V-acid sites and that suggested by Gasior et al. [4] to Bronsted acid sites on side faces of V_2O_5 crystals. Inomata et al. [5] and recently Topsoe et al. [6,7] propose mechanism involving both Bronsted acid sites and vanadyl groups. Chen and Yang [8] have found that alkali metals poisoning Bronsted acid sites caused decrease of the catalyst activity in SCR of NO. Yin et al. [9] performed DFT study of water adsorption on the basal surface of V_2O_5 crystals. Their study has showed that water could relatively easily adsorb on Lewis sites as well as vanadyl and bridging oxygen atoms, but dissociation of water on this surface did not occur.

* Corresponding author. Tel.: +48-126336377/ext. 2023; fax: +48-126340515.
E-mail address: broclawi@chemia.uj.edu.pl (E. Broclawik).

1381-1169/01/$ – see front matter
PII: S1381-1169(00)00462-3

Vanadium based catalysts usually are supported on anatase being metastable polymorph of TiO_2. Anatase supported vanadia-tungsta catalysts are known to have a wider temperature window for SCR activity than anatase supported vanadia ones [1,10]. They become active at temperatures about 100 K lower than vanadia catalysts do. Industrial $V_2O_5/WO_3/TiO_2$ catalysts contain usually about 1% w/w of V_2O_5, and about 10% w/w of WO_3 [11]. In that system, surface species are consider to be nearly isolated monomeric vanadyls and tungstyls, polymers, fragments of two dimensional monolayer or small crystals. The lowering of the onset temperature for the SCR of NO_x is usually ascribed to the higher concentration of the Bronsted acid sites on the surface of the mixed vanadia-tungsta species and the higher proton acidity of these sites [10].

The Bronsted acid site creation could occur via water dissociation on catalyst surface. We assume that tungsten might replace vanadium in V_2O_5 structure forming WO_3–V_2O_5 solid solution, similarly as it was found for molybdenum [12]. This study concerns quantum chemical modeling of water adsorption on basal surface of WO_3–V_2O_5 solid solution. After Nat. Bur. Standards Circ. [13], we call this surface (0 0 1) and assume that the same atom arrangement occurs in two-dimensional polymeric surface species due to good crystallographic fit between that surface and (0 0 1) as well as (1 0 0) ones of anatase [14]. The study was undertaken in order to validate the hypothesis that the presence of W atoms on (0 0 1) surface of the vanadia-like surface species facilitates low temperature water dissociation.

2. Computational techniques

DFT methodology and small local clusters of finite size were already shown to perform reasonably well for transition metal oxides, as well diatomic molecules as models of bulk oxides where the atoms couple via local covalent bonding with some admixture of ionic bonding [10,15–20]. The structure of V_2O_5 surface is very complicated and its full description requires a sizeable cluster model. It has been already shown that V–O bonds have fairly local character and electronic properties of vanadium sites and vanadyl or bridging oxygens do not change substantially with the cluster enlargement from $V_2O_9H_8$ to $V_{16}O_{49}H_{18}$ [18]. In view of the main goal of this study, which concerns the influence of the neighboring cation (W or V in various oxidation states) on water interaction with the cation and its nearest oxygen ligands, we have focused on small clusters representing two adjacent metal sites and bridging oxygen.

Quantum chemical calculations were done with the use of modern electronic structure methodology based on the density functional theory (DFT). For the calculations the program package DMol of Molecular Simulations, Inc. [21] was applied.

Geometry optimization procedure was used to determine the minimum-energy structure of a molecule, starting from initial geometry guess. Other properties were computed after the geometry has been minimised. Geometry optimization procedure was performed with standard parameters: medium grid, SCF density convergence, optimization energy convergence and gradient convergence equal to 0.001, 0.00001 and 0.01 a.u., respectively. Electron exchange and correlation was described by the local spin density approximation based on the Vosco, Wilk and Nusair publication [22]. As the basis set, double numerical basis functions supplemented by polarization functions (DNP) provided by the program package, was chosen equivalent to split-valence double-zeta plus polarization basis set quality, accepted as the standard basis set in quantum chemistry. The inner core of optimised atoms was frozen. The clusters with closed-shell systems were optimised using spin parameters which force both alpha and beta electrons into the same orbital. For open-shell systems, the unrestricted environmental parameter which allows electrons with different spins to use different orbitals was applied. The redox conditions were changed by using various charge parameters. For detailed energetical considerations which include determination of water binding energies on various sites and energetical features of water dissociation reaction, we have extended our calculational scheme by including nonlocal gradient corrected exchange-correlation functional BPW91 with Becke exchange [23] and Pardew–Wang correlation [24]. In this series of calculations we assumed LDA optimised geometries for each point and performed GGA energy calculations with selfconsistent potential and electron density.

3. Cluster modeling

The calculations were performed for small clusters representing two adjacent metal sites in pentacoordinated oxygen environment, analogous to bipiramidal clusters introduced in description of the (0 0 1) surface of vanadium pentoxide [18]. Cluster models were constructed to mimic surface vanadia-like species formed in the process of oxidation-induced cation segregation in V_2O_5–WO_3 solid solution [25].

Thus, the basal $V_2O_9H_8$ cluster was selected as a working model of the vanadia-like surface species [26]. In this cluster, two structurally inequivalent oxygen sites, terminal vanadyl oxygen and double bridging oxygen were represented. These oxygen atoms are present at the (0 0 1) V_2O_5 surface. Other triple bridging peripheral oxygens were artificially saturated by hydrogen atoms, thus they could not be described by our model. Geometrical structure of the $V_2O_9H_8$ cluster was fully relaxed and optimised. This unit was assumed as the model of the vanadia species formed on V_2O_5–WO_3 solid solution crystals as a result of oxidation-induced cation segregation. The subunit built of vanadyl groups and bridging oxygen seems to be a reasonable local representation of this part of V_2O_5 surface since its geometry agrees well with crystallographic data [27] (Table 1), and the frequencies of the modes of V=O, as well as VOV, are reproduced [26]. The clusters with VWO_9H_8 formula would represent other possible units of the surface species. The geometry of these clusters was reoptimised.

The other crucial factor in cluster modeling of the solid is the number of electrons in the cluster. In vanadium pentoxide vanadium and oxygen atoms take V^{5+} and O^{2-} oxidation numbers which gives null overall charge on the cluster provided that dangling bonds are saturated with protons (H^+). Substitution of W^{6+} for V^{5+} would render the cluster charge equal to +1. It is frequently assumed, however, that introducing M^{6+} into the V_2O_5 lattice is accompanied by reduction of vanadium from V^{5+} to V^{4+} to maintain lattice neutrality [12]. Thus, finally the calculations were carried out for the clusters: $[V^{5+}V^{5+}O_9H_8]^0$, $[V^{5+}V^{4+}O_9H_8]^-$, $[V^{4+}V^{4+}O_9H_8]^{2-}$ (with bond lengths and angles for saturating hydrogens fixed at the values obtained for the $[V_2O_9H_8]$ cluster), $[V^{5+}W^{6+}O_9H_8]^+$ and $[V^{4+}W^{6+}O_9H_8]^0$ (constrains from $[VWO_9H_8]$ one).

To check validity of chosen clusters as models of the V-W-O catalysts surface, the vibrational analysis was performed for all clusters and compared with the experimental Raman spectra [28]. In all cases, wavenumbers corresponding to vibrational modes of V=O and W=O were well-resolved and decoupled from other vibrations. Close inspection of the Raman spectra recorded for vanadia-tungsta showed that our calculations reproduced shifts in V=O and W=O Raman frequencies induced by the experimental changing redox conditions [28,29]. The agreement of the frequencies calculated from the cluster models with the experimental ones supports the choice of bipiramidal V-W-O clusters as the representative models of the surface species in the V-W-O catalysts, obtained by surface vanadium segregation from the V_2O_5–WO_3 solid solution in oxygen containing atmosphere.

Table 1
Calculated and crystallographic structural parameters of V–O–V subunit in V_2O_5

	DFT calculations	Crystallographic data [28]
$d_{V=O}$ (Å)	1.58	1.58
$d_{V-O\,bridge}$ (Å)	1.78	1.88

4. Results and discussion

4.1. Water adsorption

The process of water adsorption was modeled in the following way: one water molecule was placed in the vicinity of specified metallic center or on vanadyl oxygen (Fig. 1) and the geometry of the system was again reoptimised within the same scheme. The other prospective adsorption site pointed out, e.g. by Yin et al. [9], namely, double coordinated bridging oxygen, emerged as the final structure in selected optimization conditions (vide infra).

The calculations were performed for five cluster models defined above with H_2O molecule positioned either on vanadium (tungsten) site or on vanadyl (tungstyl) oxygen, which gives altogether fourteen model calculations. The binding energy (BE) of the water on the cluster served as the indicator of the

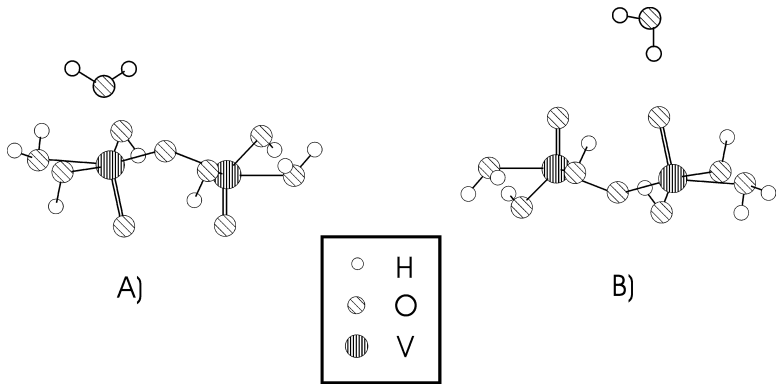

Fig. 1. Initial geometrical structures for water adsorption on $[V_2O_9H_8]$ cluster: (A) on vanadium site, (B) on vanadyl group.

system stability. It was estimated within nonlocal approximation from the total energy difference between the composed system and the sum of isolated water molecule and the cluster.

Table 2 shows water to cluster binding energies for various binding sites described above. The table is arranged in a following way: metal adsorption sites are placed in the first part of the table, while wandyl/tungstyl groups follow in the second part. The ordering remains in line with subsequent oxidation of the model vanadia cluster followed by tungsten insertion. In the cluster labelling, we use the following notation: the water molecule is placed in parenthesis next to the metal ion with which it is bound; in the case when doubly bonded terminal oxygen is the bonding site, the appropriate group is placed as a subscript of the water formula. In columns 3 and 4 bonding distances between water oxygen and a metal site, or water hydrogen pointing towards the bridging oxygen and this oxygen are given, respectively.

In the case of pure vanadia, non-negligible water binding energy emerged only for the reduced clusters. The strongest binding occurs for the water molecule interacting by hydrogen bonding with vanadyl groups. This remains in agreement with the previous studies indicating at the vanadyl oxygen as the preferred adsorption site for water in vanadia system [9]. Substitution of the tungsten in the place of the vanadium

Table 2
Binding energies (BE) and selected geometrical parameters for various adsorption modes of water on model clusters

Cluster label	BE nonlocal (kcal/mol)	V(W)–$O_{(H_2O)}$ distance, R_{VO} (Å)	$O_{bridging}$–O_{H_2O} distance, R_{OH} (Å)
$[V^{4+}V^{4+}(H_2O)O_9H_8]^{2-}$	−9.2	3.47	1.76
$[V^{5+}V^{4+}(H_2O)O_9H_8]^{-}$	−3.8	3.31	1.76
$[V^{5+}V^{5+}(H_2O)O_9H_8]^{0}$	1.0	2.64	1.93
$[V^{4+}(H_2O)W^{6+}O_9H_8]^{0}$	2.5	2.80	1.94
$[V^{4+}W^{6+}(H_2O)O_9H_8]^{0}$	0.3	2.46	1.94
$[V^{5+}(H_2O)W^{6+}O_9H_8]^{+}$	−0.7	2.33	2.49
$[V^{5+}W^{6+}(H_2O)O_9H_8]^{+}$	−8.8	2.38	2.49
$[V^{4+}V^{4+}(H_2O_{V=O})O_9H_8]^{2-}$	−21.9	–	–
$[V^{5+}V^{4+}(H_2O_{V=O})O_9H_8]^{-}$	−11.2	–	–
$[V^{5+}V^{5+}(H_2O_{V=O})O_9H_8]^{0}$	−3.6	–	–
$[V^{4+}(H_2O_{V=O})W^{6+}O_9H_8]^{0}$	−5.4	–	–
$[V^{4+}W^{6+}(H_2O_{W=O})O_9H_8]^{0}$	−4.3	–	–
$[V^{5+}(H_2O_{V=O})W^{6+}O_9H_8]^{+}$	1.1	–	–
$[V^{5+}W^{6+}(H_2O_{W=O})O_9H_8]^{+}$	−0.2	–	–

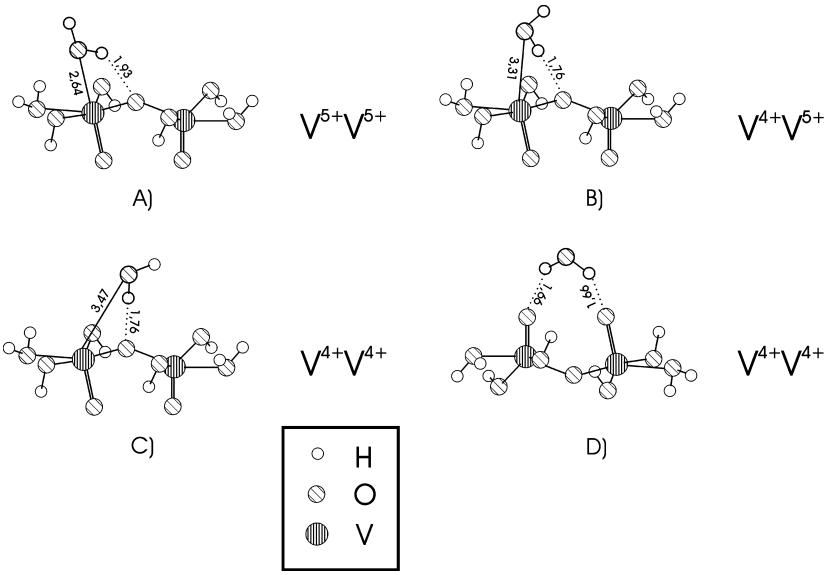

Fig. 2. Final geometries of water adsorbed on: (A) $[V^{5+}V^{5+}(H_2O)O_9H_8]^0$; (B) $[V^{5+}V^{4+}(H_2O)O_9H_8]^-$; (C) $[V^{4+}V^{4+}(H_2O)O_9H_8]^{2-}$; (D) $[V^{4+}V^{4+}(H_2O_{V=O})O_9H_8]^{2-}$.

enhances the stability of the water bound to the metal ion for the oxidised system, and weakens this bonding with reduced cluster. The bonding of the water on double bonded oxygens in mixed clusters is much weaker then in pure vanadia ones. Inspection of the binding energies described in Table 2 leads to the conclusion, that stable water binding may occur on the metal site in the case of reduced vanadia or oxidised vanadia-tungsta system. Also vanadyl groups bind water strongly.

From the point of view of the prospective water dissociation, metal ions serving as the adsorption sites seem to play the crucial role. They should host the OH group produced after the dissociation of the water molecule, while the other fragment (H or H^+) should be bonded by one of the oxygen sites on the surface. Thus, only the two clusters ($[V^{4+}V^{4+}(H_2O)O_9H_8]^{2-}$ and $[V^{5+}W^{6+}(H_2O)O_9H_8]^+$) provide prospective models for the study of the water dissociation.

However, the other critical factor influencing prospective water dissociation is the adsorption geometry. Inspection of columns 3 and 4 (Table 2) indicates that the contribution of covalent bonding realised by the lone pair donation from the water oxygen to the metal site versus hydrogen bonding of the water to the bridging cluster oxygen evolves smoothly over the studied series. For the most strongly bound system composed of the water molecule on the fully reduced vanadia cluster, the hydrogen bonding is clearly the only contribution (see also Fig. 2C). On the other side, we may assume that for the water bound strongly to the $V^{5+}W^{6+}$ clusters also the covalent contribution becomes meaningful. Thus, the dissociation process should be the most facile on the cluster $[V^{5+}W^{6+}(H_2O)O_9H_8]^+$, leading to the proton positioned on the bridging oxygen and the hydroxyl group bonded to the tungsten site. In order to validate this hypothesis, we have undertaken direct calculations of the water dissociation mechanism described in the following paragraph.

4.2. Water dissociation

To check the possibility of the water dissociation on the vanadia-tungsta solid solution surface, the preliminary dissociation of H_2O was assumed with the proton bonded to the bridging oxygen and the OH group situated on the metallic site. Geometry optimization was repeated to probe stability of the dissociated system and possible recombination of the water. The calculations were performed for five cluster models defined

in paragraph 3 with the OH group positioned either on vanadium or on tungsten site.

Calculations showed that indeed the dissociated water remained stable only in the case of the tungsten substitution, with the OH group bound to the tungsten ion. For the two clusters modeling Bronsted acid sites created after water dissociation ($[V^{4+}W^{6+}(OH)O_9H_9]^0$ and $[V^{5+}W^{6+}(OH)O_9H_9]^+$), the vibrational analysis was performed in order to probe their strength. The modes characterised by wavenumbers of the O–H bond in the W–OH group were well-isolated and were equal to 3696 and 3647 cm^{-1} for $V^{4+}W^{6+}$ and $V^{5+}W^{6+}$ clusters, respectively. This may suggest that in oxidising atmosphere, causing surface vanadium segregation [28], stronger Bronsted sites can be created on the V-W-O catalyst surface. In other cluster systems geometry optimization initiated from the preliminary dissociated water with the proton bonded to the bridging oxygen and the OH group situated on a metallic site rebuilt the cluster with covalently adsorbed water on the metal site.

In the next step, nonlocal calculations of full reaction profiles for the water dissociation have been undertaken for all models where the molecule was adsorbed on the metallic site as the adsorption on the vanadyl/tungstyl oxygen or on bridging one did not provide feasible reaction pathway. Starting geometries were taken from the optimised adsorbed systems. The choice of a proper reaction coordinate for the process with an intricate mechanism such as catalytic bond cleavage is by no means a simple task. Here, two geometrical coordinates are evidently crucial for OH dissociation: intramolecular OH distance in water and the distance between selected dissociative hydrogen and bridging oxygen from the cluster. Thus, the dissociation path should be in principle described on two-dimensional potential energy surface, which is calculationally very demanding in the case of transition metal oxide cluster models. Our previous experience [16,30] showed that the energy profile for X–H bond dissociation in the molecule interacting with transition metal oxide surface could be effectively described by assuming the angle X–metal–H as the reaction coordinate. In this work, we have taken the angle O_{H_2O}–metal–H_{H_2O} as the geometrical parameter governing the process of water dissociation. Starting from the stable adsorption geometry, the angle was incremented every 4° and the other geometrical parameters were optimised within LDA approximation for each point at the reaction profile, with constraints common for all our model calculations. Then, the total energy was recalculated within NLDA scheme.

Fig. 3 shows the two representative reaction profiles obtained in this study: for the $[V^{5+}V^{5+}(H_2O)O_9H_8]^0$ and $[V^{5+}W^{6+}(H_2O)O_9H_8]^+$ systems. The energy was scaled with respect to separate cluster and free water molecule taken as the zero level in each case thus the adsorption energy could be directly measured at each stage of the reaction. The curves on Fig. 3 were interpolated by polynomials to obtain R^2 value >0.99. In the first case, energy rose monotonously along the reaction profile and no second energy minimum was spotted which would correspond to stable dissociated system. For analogous tungsten substituted system

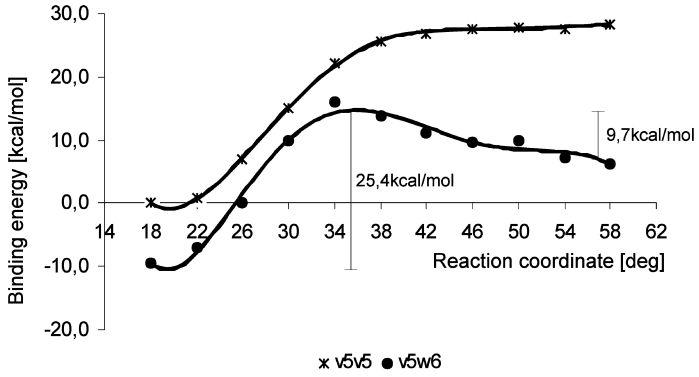

Fig. 3. Energy profiles for dissociation reaction of water on $[V^{5+}V^{5+}(H_2O)O_9H_8]^0$ (v5v5) and $[V^{5+}W^{6+}(H_2O)O_9H_8]^+$ (v5w6) clusters (dissociation and recombination barriers are marked on second profile).

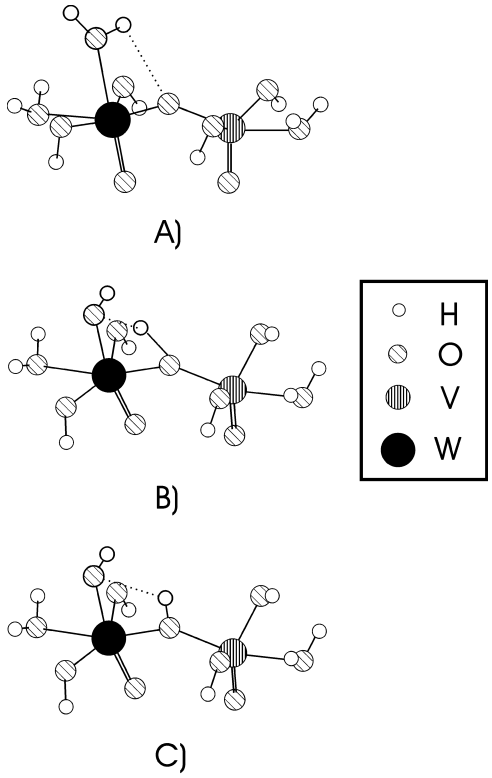

Fig. 4. Geometrical structures of adsorbed water (A), transition state (B) and dissociated water (C) for $[V^{5+}W^{6+}(H_2O)O_9H_8]^+$ system.

(second curve), the energy barrier appeared corresponding presumably to the transition state and the local energy minimum was achieved after crossing the barrier. The geometrical structure at the minimum was the one obtained previously for full optimization close to assumed dissociated structure. Geometrical structures of initial system, transition state and the final dissociated system are shown in Fig. 4.

Only for the two models with the water adsorbed on the tungsten site in a mixed V-W-O cluster dissociative energy profiles analogous to the second curve have been obtained. For all other models, nondissociative curve emerged analogous to the $[V^{5+}V^{5+}(H_2O)O_9H_8]^0$ case. Reaction profile calculations allowed for quantitative analysis of energy of catalytic water dissociation. The energetical barrier for the OH bond scission on the $V^{5+}W^{6+}$ cluster is equal to 25.4 kcal/mol, the depth of local energy minimum with respect to the transition state is 9.7 kcal/mol. The minimum describing the system after the dissociation might be regarded as a rather shallow one and its energy lies above the one of isolated subsystem. Nevertheless, one should keep in mind that the proton created after dissociation is a mobile species and could migrate to other oxygen sites on the surface, presumably preferred sites for proton adsorption [18,31]. This result fully confirmed the hypothesis that tungsten substitution is indispensable for creating conditions for effective water dissociation.

5. Conclusions

It has been already known [25,32] that the surface V segregation in oxidising conditions in V-W-O catalysts leads to enrichment of the surface in V-O-W subunits. Our model calculations showed that in these conditions, water adsorption on tungsten sites may be strengthened which leads to enhanced probability of the dissociation of water molecule producing Bronsted acidic sites. Indeed, in oxidising conditions, the water adsorption on tungsten sites in the mixed V-W-O clusters is strong enough to prevail over vanadium or vanadyl sites and, at the same time, energetical barrier for the dissociation is low enough to enable dissociation. Stability of the dissociated system was found to be only a few kcal/mol with respect to the barrier and the recombination of molecularly adsorbed water could also occur.

Water can adsorb on V_2O_5 Lewis sites but creating the Bronsted acidic sites is not allowed. Our data seem to provide a good verification of the hypothesis that tungsten atoms in WO_3–V_2O_5 solid solution increase concentration of the Bronsted acid sites on the surface. The lowering of the onset temperature of SCR of NO_x by tungsten addition can be ascribed to the formation of the VW sites active in low temperature dissociative water adsorption. Increase in the low temperature SCR activity with increase of O_2 content [33] in reacting gases or with preliminary catalyst oxidation [29] may be attributed to the formation of $[V^{5+}W^{6+}O_9H_8]^+$ units of WO_3–V_2O_5 solid solution with Bronsted acid sites of high protonic acidity.

Acknowledgements

This work was sponsored by Polish Committee of Scientific Research (KBN) (PB 0820/T 09/96/11).

References

[1] G. Busca, L. Lietti, G. Ramis, F. Berti, Appl. Catal. B 18 (1998) 1.
[2] F. Janssen, F. van ded Kerkhof, H. Bosch, J.J. Ross, Phys. Chem. 91 (1987) 6633.
[3] G. Ramis, G. Busca, F. Bregani, P. Forzatti, Appl. Catal. 64 (1990) 259.
[4] M.G. Gasior, J. Haber, T. Machej, T. Czeppe, J. Mol. Catal. 43 (1988) 359.
[5] M. Inomata, A. Miyamoto, Y. Murakami, J. Catal. 40 (1980) 62.
[6] N.Y. Topsoe, H. Topsoe, J.H. Dumesic, J. Catal. 151 (1995) 226.
[7] J.A. Dumesic, N.-Y. Topsoe, H. Topsoe, Y. Chen, T. Slabiak, J. Catal. 163 (1996) 409.
[8] J.P. Chen, R.T. Yang, J. Catal. 125 (1990) 411.
[9] X. Yin, A. Fahmi, H. Han, A. Endou, S.S.C. Ammal, M. Kubo, K. Teraishi, A. Miyamoto, J. Phys. Chem. B 103 (1999) 3218.
[10] J.P. Chen, R.T. Yang, Appl. Catal. A 80 (1992) 135.
[11] L.J. Alemany, F. Berti, G. Busca, G. Ramis, D. Robba, G.P. Toledo, M. Trombetta, Appl. Catal. B 248 (1996) 299.
[12] A. Bielanski, M. Najbar, Appl. Catal. A 157 (1997) 223.
[13] Nat. Bur. Standards Circ. 539, PDF 9-387, JCPDS (8) (1958) 66–67.
[14] A. Vejux, P. Courtine, J. Solid State Chem. 23 (1978) 93.
[15] E. Broclawik, D.R. Salahub, J. Mol. Catal. 82 (1993) 117.
[16] E. Broclawik, in: J.M. Seminario, P. Politzer, (Eds.), Modern Density Functional Theory: A Tool for Chemistry, Elsevier, Amsterdam, 1995, p. 349.
[17] J. Haber, M. Witko, R. Tokarz, J. Mol. Catal. 66 (1991) 205.
[18] A. Michalak, M. Witko, K. Hermann, Surf. Sci. 375 (1997) 385.
[19] K. Herman, A. Michalak, M. Witko, Catal. Today 32 (1996) 321.
[20] M. Witko, Catal. Today 32 (1996) 89.
[21] DMol, Insight II release 95.0, Biosym/MSI, San Diego, 1995.
[22] S.H. Vosco, L. Wilk, M. Nusair, Can. J. Phys. 58 (1990) 1200.
[23] A.D. Becke, Phys. Rev. A 38 (1988) 3098.
[24] J.P. Perdew, Y. Wang, Phys. Rev. B 45 (1992) 13244.
[25] M. Najbar, J. Camra, Solid State Ionics 101–103 (1997) 707.
[26] A. Góra, E. Broclawik, M. Najbar, Comput. Chem. 24 (2000) 405.
[27] R. Enjalbert, J. Galy, Acta Crystallogr. Sect. C: Cryst. Struct. Commun. 42 (1986) 1467.
[28] M. Najbar, E. Broclawik, A. Góra, J. Camra, A. Bialas, A. Weselucha-Birczynska, Phys. Chem. Phys. Lett. 325 (2000) 330.
[29] M. Najbar, F. Mizukami, A. Bialas, J. Camra, A. Weselucha-Birczynska, H. Izutsu, A. Góra, Top. Catal. 11/12 (2000) 131.
[30] E. Broclawik, Density functional theory in catalysis: activation and reactivity of a hydrocarbon molecule on a metallic active site, Adv. Quant. Chem. 33 (1999) 349.
[31] M. Witko, K. Herman, R. Tokarz, Catal. Today 50 (1999) 553.
[32] M. Najbar, J. Camra, A. Bialas, A. Weselucha-Birczynska, B. Borzecka-Prokop, L. Delevoye, J. Klinowski, Phys. Chem. Chem. Phys. 1 (1999) 4645.
[33] L. Lietti, I. Nova, E. Tronconi, P. Forzatti, AIChE J. 43 (10) (1997) 2559.